33rd Annual International Conference of the IEEE EMBS
Boston, Massachusetts USA, August 30 - September 3, 2011

Atheromatic™: Symptomatic vs. Asymptomatic Classification Of Carotid Ultrasound Plaque using a combination of HOS, DWT & Texture

U Rajendra Acharya, Oliver Faust, Vinitha Sree S., Ang Peng Chuan Alvin, Ganapathy Krishnamurthi, Jos´e C. R. Seabra, João Sanches, Jasjit S Suri, *Sr. Member, IEEE, Fellow, AIMBE*

***Abstract*—Quantitative characterization of carotid atherosclerosis and classification into either symptomatic or asymptomatic is crucial in terms of diagnosis and treatment planning for a range of cardiovascular diseases. This paper presents a computer-aided diagnosis (CAD) system (Atheromatic™, patented technology from Biomedical Technologies, Inc., CA, USA) which analyzes ultrasound images and classifies them into symptomatic and asymptomatic. The classification result is based on a combination of discrete wavelet transform, higher order spectra and textural features. In this study, we compare support vector machine (SVM) classifiers with different kernels. The classifier with a radial basis function (RBF) kernel achieved an accuracy of 91.7% as well as a sensitivity of 97%, and specificity of 80%. Encouraged by this result, we feel that these features can be used to identify the plaque tissue type. Therefore, we propose an integrated index, a unique number called symptomatic asymptomatic carotid index (SACI) to discriminate symptomatic and asymptomatic carotid ultrasound images. We hope this SACI can be used as an adjunct tool by the vascular surgeons for daily screening.**

***Index Terms*—atherosclerosis, symptomatic, carotid, higher order spectra, texture, discrete wavelet transform, classifier, support vector machine.**

I. Introduction

HEART disease and stroke are mainly due to occlusion due to atherosclerosis and high blood pressure [1]. Stroke remains the third most common cause of death in most industrialized countries. Atherosclerosis is a condition of thickening of artery due to deposition of multiple plaques [2]. It has been shown that surgical removal of plaques reduced the risk of ipsilateral stroke [3]. Since not all carotid plaques are necessarily harmful and as carotid surgery carries a considerable risk for the patient, optimized diagnosis and patient selection is of paramount importance. For both surgery and treatment, an early detection of carotid atherosclerosis plaque and the classification of the same into symptomatic [4] or asymptomatic [5] are crucial. Invasive methods like intravascular ultrasound [6], [7] carry risks. Non-invasive carotid artery ultrasound is also well established but the correlation between ultrasonographic features and the histological evaluation of carotid plaques is often poor [8], [9]. Improving the ultrasound image quality with adequate preprocessing as well as extracting discriminate features will increase the correlation between automated classification results and histological results of carotid plaques. In this paper, we present an effective texture derived atherosclerotic tissue characterization algorithm which can be used in CAD systems. We call the system as Atheromatic™ (Patented Technology from Global Biomedical Technologies, Inc., California, USA). The block diagram, in Fig. 1, shows the structure of the algorithm.

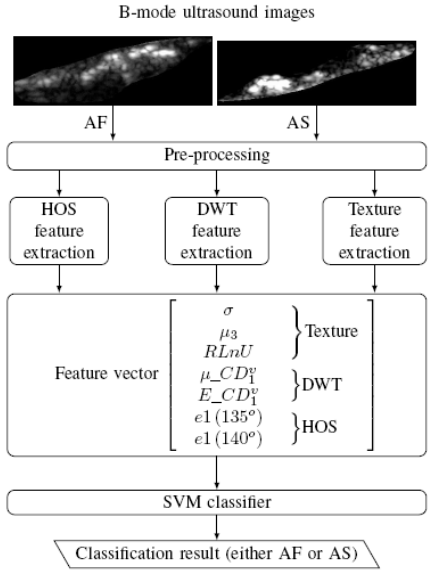

Fig 1. Block diagram of the proposed system

II. Materials and Methods

A. Carotid ultrasound image acquisition and preprocessing

Data include 146 carotid bifurcation plaques from 99 patients, 75 males and 24 females. Mean age was 68 years old (41-88). Patients were observed consecutively through neurological consultation which included non-invasive examination with color-flow duplex scan of one or both carotids. A plaque was considered symptomatic when Amaurosis fugax or focal transitory, reversible or established neurological symptoms in the ipsilateral carotid territory, were observed in the previous 6 months. 110 plaques were identified as asymptomatic while 50 have shown symptoms.

Manuscript received December 8, 2010.

U. R. Acharya, O. Faust and A.P.C Alvin are with the Department of Electrical and Computer Engineering, Ann Polytechnic, Singapore 599489, e-mail: aru at np.edu.sg, fol2 at np.edu.sg .

Vinitha Sree S is with the School of Mechanical and Aerospace Engineering, College of Engineering, Nanyang Technological University, 50, Nanyang Avenue, Singapore 639798

Jo˜ao Sanches and Jos´e C. R. Seabra are with the Department of Electrical and Computer Engineering, Instituto Superior T´ecnico, Portugal

Ganapathy Krishnamurthi is with the Case Western Reserve University in Cleveland, OH, USA

Jasjit S Suri with the Global Biomedical Technologies Inc., California, USA & Idaho State University (Aff.), ID, USA, jsuri at comcast.net

Image normalization was achieved as previously reported [10]; hence, the image intensities were linearly scaled so that the adventitia and blood intensities would be in the range of 190-195 and 0-5, respectively.

The normalized image is used to segment existing plaque(s) in the image. Speckle free and Speckle components were extracted as described in [11,12].

B. Texture Features

Texture is defined as a regular repetition of an element or pattern in a surface structure [13]. We use the following statistical texture features, Deviation (standard deviation), the third moment of the Co-Occurrence Matrix, Run Length Non uniformity (RnLU) [14,15].

C. Discrete Wavelet Transform Features

In both numerical and functional analysis, a DWT is any wavelet transform for which the wavelets are discretely sampled [16]. A key advantage over the well known Fourier transforms [17] is temporal resolution: it captures both frequency and location information (position in time).

The two-dimensional DWT (bi-orthogonal wavelet) leads to a decomposition of approximation coefficients at level j in four components: the approximation CA_{j+1} at level $j+1$, and the details in three orientations (horizontal CD^{h}_{j+1}, vertical CD^{v}_{j+1}, and diagonal CD^{d}_{j+1}).

We have used the average intensity and average energy of CD^{v}_{1} as the first DWT feature:

$$AVERAGE\_CD_1^v = \sum_{<j>}\sum_{<i>} CD_1^v(i,j) \quad (1)$$

The second DWT feature was defined as the energy of CD^{v}_{1}.

$$AVERAGE\_CD_1^v = \sum_{<j>}\sum_{<i>} \left(CD_1^v(i,j)\right)^2 \quad (2)$$

D. Higher Order Spectra (HOS)

Bi-spectrum phase entropy [18], [19], [20] is another feature used. In this study we have used the phase entropy on the radon transform [21] for $\theta = 135^0$ and $\theta = 140^0$ of the B-mode ultrasound images. This yields two features: $e1(135^0)$ and $e1(140^0)$.

E. Classification using Support Vector Machines (SVM)

The SVM is a maximum margin classifier *i.e.,* it maximizes the distance between the decision hyperplane and the closest class training data called support vectors. Initially designed for two class problems, it has been extended for multiclass as well [22, 23, 24]. Five standard kernels were used for classification. The linear kernel, polynomial kernel of order 1, 2 and 3 and the Radial Basis Function Kernel were used.

III. RESULTS

The three-fold stratified cross validation method was used to evaluate the classifier performance [25]. Two thirds of the data were used for training and the remaining one third was used to test the performance. This procedure was repeated three times using different folds of the test data each time. Subsequently, we calculated the accuracy, sensitivity, specificity, positive predictive value (PPV), and AUC by averaging the values obtained in three iterations.

A. Statistical results

Table I depicts the result of texture features extracted from the carotid images. This table indicates the features used for classification, and their respective mean and standard deviation values and p-values for symptomatic and asymptomatic cases respectively. All seven features are clinically significant as they show low p-values (< 0.01).

TABLE I T-TEST RESULTS FOR DWT, HOS AND TEXTURE FEATURES

Features	Symptomatic	Asymptomatic	P value
σ	32.8 ± 9.57	37.9 ± 11.0	0.0046
μ_s	2.93 ± 1.32	2.39 ± 0.98	0.0047
RLnU	4.083 E+03 ± 1.114E+03	2.653 E+03 ±546	< 0.0001
$\mu\_CD_1^v$	5.034E-02 ± 1.248E-02	4.477E-02 ±1.140E-02	0.0060
$E\_CD_1^v$	6.500E-08 ± 1.695E-08	5.758E -08 ± 1.579E -08	0.0078
$e1(135^0)$	1.59±0.536	2.04 ±0.644	< 0.0001
$e1(140^0)$	1.18 ± 0.399	1.56 ±0.732	0.0008

B. SVM Results

In this work, we have used 112 plaque images (35 symptomatic and 77 asymptomatic) for training and 48 plaque images for testing (15 symptomatic and 33 asymptomatic). The classification results obtained using different SVM kernel configurations are shown in Table II. It can be seen that the SVM classifier with the RBF kernel presented the highest performance measures (Accuracy: 91.7%; Sensitivity: 97%; Specificity: 80%; AUC: 0.885) among all the other SVM configurations. The ROC curves obtained for all SVM configurations are depicted in Fig. 2. As seen from the ROC curves, the SVM classifier with the RBF kernel function is the better classifier amongst the rest as it has the highest AUC of 0.885.

C. Index results

We have shown how well the seven features differentiate symptomatic and asymptomatic plaque formations in B-mode ultrasound images. However, it is difficult and time-consuming to track how these seven indices vary in a patient for making an appropriate diagnosis. Hence, we combined the

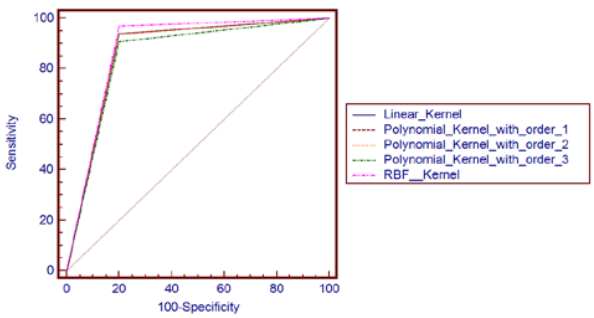

Fig. 2 ROC curves for various SVM kernels

features in such a way that the index value for symptomatic is distinctly different from the value resulting from asymptomatic plaque formations. This novel integrated index, termed Symptomatic Asymptomatic Carotid Index (SACI), is calculated using the following equation.

$$SACI = 2.\log_{10}(RLnU) - \frac{\log_{10}\left(R1 - R2 * R3\right)}{5}$$

$$R1 = \log_{10}\left(\frac{AVERAGE\_CD_1^v}{ENERGY\_CD_1^V}\right) \quad (3)$$

$$R2 = Deviation \times Third\_Moment$$

$$R3 = e1(135^0) \times e1(140^0)$$

Fig.3 shows the range of SACI for symptomatic and asymptomatic carotid ultrasound images. These values are clinically significant because the p-value is very low (< 0:0001).The spread of the SACI for symptomatic and symptomatic classes is distinct.

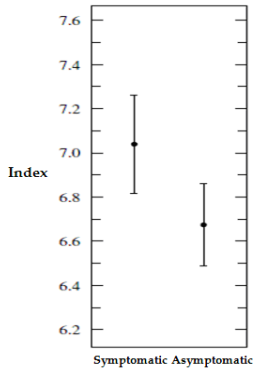

Fig. 3 Box plot of the SACI index

IV. DISCUSSION

Kyriacou et al., (2009) studied the usefulness of multilevel binary and gray scale morphological analysis in the assessment of atherosclerotic carotid plaques [26]. SVM and probabilistic neural network were applied to pattern spectra from US images to classify into either a symptomatic or an asymptomatic class. The highest percentage of correct classifications score was 73.7% for multilevel binary morphological image analysis and 66.8% for gray scale morphological analysis. Both were achieved using the SVM classifier.

Recently, Seabra et al. [27] proposed a method for plaque characterization based on a de-speckling algorithm, resulting in features extracted from de-speckled and speckle image sources. In this study, the use of textural information for correct identification of different plaque types was reinforced. They obtained an almost perfect classification result in terms of sensitivity and accuracy. A direct comparison with their results is not possible because of the difference in the feature space. However they do show a sensitivity of 90% when using only texture and histogram features computed from normalized BUS images which is comparable to our results. We were able to achieve 97% sensitivity based on a limited number of features extracted automatically. We believe that our classifier performance will improve with the addition of more relevant features.

TABLE II CLASSIFICATION RESULTS WHERE TN IS TRUE NEGATIVE, FN IS FALSE NEGATIVE, TP IS TRUE POSITIVE, AND FP IS FALSE POSITIVE

SVM	TN	FN	TP	FP	Accuracy	PPV	Sensitivity	Specificity	AUC
Linear Kernel	12	2	31	3	89.6%	90.7%	94.9%	77.8%	0.870
Polynomial Kernel with order 1	12	2	31	3	89.6%	90.7%	94.9%	77.8%	0.870
Polynomial Kernel with order 2	12	2	31	3	89.6%	91.6%	93.9%	80%	0.870
Polynomial Kernel with order 3	12	3	30	3	86.1%	90.8%	89.9%	77.8%	0.855
RBF Kernel	12	1	32	3	91.7%	91.8%	97%	80%	0.885

Our preliminary results suggest that HOS features are very powerful features that lead to improvement in classification.

The AUC shows that the RBF kernel gives the best performance. The RBF kernel can be expanded in to an infinite series giving rise to an infinite dimensional polynomial kernel. Each of these polynomial kernels can then transform certain dimensions to make them linearly independent.

We have shown how well the index can differentiate symptomatic and asymptomatic plaque subjects. A novel approach, as in [28, 29], of formulating an index by combining the parameters in such a way that the index values are distinctly different for symptomatic and asymptomatic was used. We computed the values of this *SACI* for symptomatic and asymptomatic (Fig. 3). It can be clearly seen, from this plot that our integrated index can be employed to effectively differentiate and diagnose symptomatic and asymptomatic plaque classes. These ranges are unique and clinically significant ($p<0.0001$). The Index can also be employed to assess the efficacy of plaque medication.

V. CONCLUSION

Plaque identification from B-mode ultrasound images is very a difficult task. Hence, we have used advanced texture, DWT features and HOS information (Bispectrum) coupled with the SVM algorithm to classify symptomatic and

asymptomatic plaques. The proposed CAD system (Atheromatic^{TM}) may be a valuable tool which helps to optimize the clinical work flow, since it provides decision support with regard to carotid plaque treatment. The system is able to diagnose the two types of plaque formations automatically with an accuracy of more than 86%. Furthermore, a symptomatic asymptomatic carotid index has been proposed to identify the plaque formation in carotid ultrasound images using a single number. This paves way for a more objective diagnosis methodology.

REFERENCES

[1] D. R. Labarthe, Epidemiology and Prevention of Cardiovascular Diseases: A Global Challenge. An Aspen Publication, 1998.

[2] A. Maton, R. L. J. Hopkins, C. W. McLaughlin, S. Johnson, M. Q. Warner, D. LaHart, and J. D. Wright, Human Biology and Health. Prentice Hall, Englewood Cliffs, New Jersey, USA, 1993.

[3] G. G. Ferguson, M. Eliasziw, H. W. K. Barr, G. P. Clagett, R. W. Barnes, M. C. Wallace, D. W. Taylor, R. B. Haynes, J. W. Finan, V. C. Hachinski, and H. J. M. Barnett, "The North American Symptomatic Carotid Endarterectomy Trial : Surgical Results in 1415 Patients," Stroke, vol. 30, no. 9, pp. 1751–1758, 1999. [Online]. Available: http://stroke.ahajournals.org/cgi/content/abstract/30/9/1751

[4] J. Golledge, R. M. Greenhalgh, and A. H. Davies, "The Symptomatic Carotid Plaque," Stroke, vol. 31, no. 3, pp. 774–781, 2000. [Online]. Available: http://stroke.ahajournals.org/cgi/content/abstract/31/3/774

[5] J. M. Johnson, M. M. Kennelly, D. Decesare, S. Morgan, and A. Sparrow, "Natural History of Asymptomatic Carotid Plaque," Arch Surg, vol. 120, no. 9, pp. 1010–1012, 1985. [Online]. Available: http://archsurg.ama-assn.org/cgi/content/abstract/120/9/1010

[6] S. E. Nissen, E. M. Tuzcu, P. Schoenhagen, B. G. Brown, P. Ganz, R. A. Vogel, T. Crowe, G. Howard, C. J. Cooper, B. Brodie, C. L. Grines, and A. N. DeMaria, "Effect of Intensive Compared With Moderate Lipid-Lowering Therapy on Progression of Coronary Atherosclerosis: A Randomized Controlled Trial," JAMA, vol. 291, no. 9, pp. 1071–1080, 2004. [Online]. Available: http://jama.amaassn.org/cgi/content/abstract/291/9/1071

[7] J. Seabra and J. Sanches, "Modeling log-compressed ultrasound images for radio frequency signal recovery." Conf Proc IEEE Eng Med Biol Soc, vol. 2008, pp. 426–9, 2008. [Online]. Available: http://www.biomedsearch.com/nih/Modeling-log-compressed-ultrasound-images/19162684.html

[8] D. W. Droste, M. Karl, R. M. Bohle, and K. M, "Comparison of ultrasonic and histopathological features of carotid artery stenosis," Neurol Res.y, vol. 19, pp. 380 – 384, 1997.

[9] E. Ringelstein, C. Sievers, S. Ecker, P. Schneider, and S. Otis, "Noninvasive assessment of CO2-induced cerebral vasomotor response in normal individuals and patients with internal carotid artery occlusions," Stroke, vol. 19, no. 8, pp. 963–969, 1988. [Online]. Available: http://stroke.ahajournals.org/cgi/content/abstract/19/8/963

[10] T. Elatrozy, A. Nicolaides, T. Tegos, and M. Griffin, "The objective characterisation of ultrasonic carotid plaque features,"European Journal of Vascular and Endovascular Surgery, vol. 16, no. 3, pp. 223-230,1998.[Online].Available: http://www.sciencedirect.com/science/article/B6WF5-4H3SF3Y-8/2/8011fe8e92fdb924982dfc5442f916ba

[11] J. Seabra and J. Sanches, "Modeling log-compressed ultrasound images for radio frequency signal recovery." Conf Proc IEEE Eng Med Biol Soc, vol. 2008, pp. 426–9, 2008. [Online]. Available: http://www.biomedsearch.com/nih/Modeling-log-compressed-ultrasound-images/19162684.html

[12] J. Seabra, J. Xavier, and J. Sanches, "Convex ultrasound image reconstruction with log-euclidean priors." Conf Proc IEEE Eng Med Biol Soc, vol. 2008, pp. 435–438, 2008.

[13] M. Mirmehdi, X. Xie, and J. Suri, Handbook of Texture Analysis. London, UK, UK: Imperial College Press, 2009.A. Ramm and A. Katsevich, The radon transform and local tomography. CRC Press, 1996. [Online]. Available: http://books.google.com.sg/books?id=Ifce8tC7sagC

[14] M. M. Galloway, "Texture analysis using grey level run lengths," NASA STI/Recon Technical Report N, vol. 75, pp. 18, Jul. 1974.

[15] D. Xu, A. S. Kurani, J. D. Furst, and D. S. Raicu, "Run-length encoding for volumetric texture," in The 4th IASTED International Conference on Visualization, Imaging, and Image Processing, 2004.

[16] S. Mallat, A Wavelet Tour of Signal Processing, Third Edition: The Sparse Way, 3rd ed. Academic Press, 2008.

[17] S. Bochner and K. Chandrasekharan, Fourier transforms, ser. Ann. Math. Stud. Princeton, NJ: Princeton Univ. Press, 1949.

[18] K. C. Chua, V. Chandran, R. Acharya, and C. M. Lim, "Automatic identification of epilepsy by hos and power spectrum parameters using eeg signals: A comparative study," 2008. [Online]. Available: http://eprints.qut.edu.au/14787/

[19] K. Chua, V. Chandran, U. Acharya, and C. Lim, "Application of higher order spectra to identify epileptic eeg," Journal of Medical Systems, pp. 1–9, 2010, 10.1007/s10916-010-9433-z. [Online]. Available: http://dx.doi.org/10.1007/s10916-010-9433-z

[20] R. Acharya U., K. C. a. T.-C. L. Chua, Dorithy, and J. S. Suri, "Automatic identification of epileptic eeg signals using nonlinear parameters," JMMB, vol. 9, pp. 539–553, 2009.

[21] U.R. Acharya, C.K. Chua, E.Y.K. Ng, W. Yu, C.Chee, "Application of higher order spectra for the identification of diabetes retinopathy stages, "Journal of Medical Systems, vol. 32, No.6, pp. 481–488, 2008.

[22] C. Cortes and V. Vapnik, "Support-vector networks," Mach. Learn., vol. 20, pp. 273–297, September 1995. [Online]. Available: http://portal.acm.org/citation.cfm?id=218919.218929

[23] B. E. Boser, I. M. Guyon, and V. N. Vapnik, "A training algorithm for optimal margin classifiers," in Proceedings of the fifth annual workshop on Computational learning theory, ser. COLT '92. New York, NY, USA: ACM, 1992, pp. 144–152. [Online]. Available: http://doi.acm.org/10.1145/130385.130401

[24] M. A. Aizerman, E. A. Braverman, and L. Rozonoer, "Theoretical foundations of the potential function method in pattern recognition learning." in Automation and Remote Control,, no. 25, 1964, pp. 821–837.

[25] R. Kohavi, "A study of cross-validation and bootstrap for accuracy estimation and model selection," in Proceedings of the 14th international joint conference on Artificial intelligence Volume 2. San Francisco, CA, USA: Morgan Kaufmann Publishers Inc., 1995, pp. 1137-1143. [Online]. Available: http://portal.acm.org/citation.cfm?id=1643031.1643047.

[26] E. Kyriacou, M. S. Pattichis, C. S. Pattichis, A. Mavrommatis, C. I. Christodoulou, S. Kakkos, and A. Nicolaides,"Classification of atherosclerotic carotid plaques using morphological analysis on ultrasound images," Applied Intelligence, vol. 30, pp. 3–23, February 2009. [Online]. Available: http://portal.acm.org/citation.cfm?id=1485060.1485063

[27] J. Seabra, L. M. P. (MD), F. e Fernandes, and J. M. Sanches, "Ultrasonographic characterization and identification of symptomatic carotid plaques," in Engineering in Medicine and Biology Society, 2010. EMBS 2010. 32th Annual International Conference of the IEEE, September. 2010.

[28] Ghista DN. Physiological Systems' Numbers in Medical Diagnosis and Hospital Cost effective Operation. Journal of Mechanics in Medicine & Biology 2004; 4(4): 401–418.

[29] Ghista DN. Nondimensional Physiological indices for medical assessment .Journal of Mechanics in Medicine & Biology 2009; 9(4): 643-669.